4.5 PROBABILITY FORECASTS OF AIRCRAFT ICING FOR THE CONTIGUOUS U.S.

Ronald M. Reap*

Techniques Development Laboratory
Office of Systems Development
National Weather Service, NOAA

1. INTRODUCTION

This paper describes the new NGM-based probability forecasts of nonconvective aircraft icing for the contiguous U.S. that will become operational during the 1996-97 cool season. The equations to produce these forecasts were developed from forecast fields from the National Centers for Environmental Prediction's (NCEP's) Nested Grid Model (NGM) (Hoke et al. 1989), national lightning location data (Krider et al. 1976), and pilot reports (PIREPS) from the Aviation Weather Center's (AWC's) data archives. The forecast equations give the unconditional probability of category 4 (light-to-moderate) or greater aircraft icing in 48-km grid blocks covering the contiguous United States during 6-h periods valid 2-8, 8-14, 14-20, and 20-26 hours after 0000 and 1200 UTC initial data times. The new probability forecasts were designed to provide general objective guidance in the 2-26 h timeframe to forecasters at the Aviation Operations Branch of AWC located in Kansas City, Missouri. AWC is responsible for issuing operational inflight advisories (AIRMETS and SIGMETS) for use by the commercial and general aviation communities.

2. DEVELOPMENT

2.1 Method

The icing forecast equations were derived by applying screening regression techniques and the Model Output Statistics (MOS) approach (Glahn and Lowry 1972) to relate the PIREP predictand data to large-scale meteorological predictors obtained from the NGM. National lightning location data were used to eliminate icing reports arising from localized thunderstorms. As a result, the forecast equations predict the probability of occurrence of nonconvective aircraft icing. Separate equations were developed for the eastern and western U.S. to accommodate the unique meteorological conditions related to icing over the western mountains. Equations were developed for the high-band (> 15,000 ft above ground level (AGL)) and low-band (< 15,000 ft AGL) regions. Separate forecast equations were also developed for the warm season (March 16 - September 30) and cool season (October 1 - March 15) periods.

Corresponding author address: 1325 East-West Highway, Rm 10380, Silver Spring, MD 20910-3283
e-mail <Ronald.Reap@noaa.gov>

2.2 Predictand Sample

PIREP data were obtained from AWC for the 3-year period from 1988-90. Like many observed datasets, PIREPS suffer from specific limitations (Schwartz 1996). They are, however, the only practical method for determining the existence of aircraft icing. The reports are intermittent in both time and space and are relatively scarce at night when few aircraft are aloft. Reports of icing are subjective in nature and, therefore, uncalibrated since they depend upon the pilot's perception of the degree of icing. Despite these limitations, the present developmental effort was successful in using the PIREPS to identify significant areas of aircraft icing that were related to major features in the large-scale flow.

During initial processing, the reported icing events, whose positions are given by latitude and longitude in the PIREPS, were related to an 89x113 grid covering the contiguous United States. The maximum value of icing observed during the hour was tabulated and stored for each 48-km grid block in the 89x113 array, i.e., if multiple icing events were reported for an individual 48-km grid block, only the maximum value was saved. The archived icing intensity for each grid block was indicated by the category values that were originally used to encode the PIREPS, that is,

0 = None
1 = Trace
2 = Trace to Light
3 = Light
4 = Light to Moderate
5 = Moderate
6 = Moderate to Heavy
7 = Heavy
8 = Severe

In processing the PIREP data, an icing event was considered to have occurred when icing intensities of category 4 or greater were reported. All icing reports of category 4 or greater were accepted regardless of aircraft type. For an icing event with multiple latitudes and longitudes, i.e., a line segment, or dogleg in the case of three sets of latitudes and longitudes, the event was assigned to all 48-km grid blocks through which the line segment(s) passed. Line or dogleg segments over 300 mi (480 km) were, however, not used due to the likelihood of reporting errors. Aviation forecasters at AWC have observed through experience that segments over 300 mi are sometimes unreliable. In general, most line segments are reported by general aviation pilots in the low-band region at or below 15,000 ft. Above 15,000 ft, airline and military pilots usually give point reports of aircraft icing.

As previously noted, national lightning location data were used to eliminate any icing events associated with thunderstorm activity. In effect, a value of zero for the icing intensity was stored for 48-km grid blocks where one or more cloud-to-ground flashes were reported during the hour. Grid blocks immediately adjacent to a thunderstorm area were also zeroed to reduce the possibility of contaminating the sample with convective icing events.

2.3 Predictor Sample

Atmospheric conditions that lead to aircraft icing are mesoscale in nature and are not resolvable at the grid spacing of the NGM. Icing conditions are most commonly found in clouds where supercooled liquid water (SLW) is present, i.e., where the temperature range lies between 0 and -20 deg C. The threat of ice accumulation to aircraft passing through the supercooled layers is determined by the size and distribution of the cloud droplets and the speed and aerodynamic characteristics of the aircraft. Icing prediction is, therefore, a matter of identifying cloudy regions with the appropriate temperature range. In practice, forecasters have used the 850-mb temperature, 1000-500 mb mean relative humidity, and 700-mb vertical motion to delineate threat areas for icing (Schultz and Politovich 1992). The NGM predictors offered to the screening regression procedure used in the current work are, therefore, designed to identify large-scale synoptic flow patterns that are related to the occurrence of aircraft icing. This approach has been successfully employed in previous MOS developmental efforts to predict other mesoscale weather elements, e.g., clear-air turbulence (Reap 1996).

The predictor sample included a set of basic and derived predictors from the NGM. Derived predictors include potential temperature, equivalent potential temperature, temperature-dew point spread, vertical velocity times relative humidity, equivalent potential vorticity (Rotunno and Klemp 1985), and height of freezing level. Stability indices in the form of the Total Totals index (Miller 1972), K index (George 1960), and lifted index were also included. The terrain-induced vertical velocities were included to account for the generation of SLW by orographic lifting. As shown by Modica et al. (1994), orographic lifting can be responsible for producing SLW at levels near 500-600 mb over the western mountains. Also included were several predictors originally developed for the prediction of clear-air turbulence (Reap 1996), i.e., the deformation and the TI1 and TI2 indices developed by Mancuso and Endlich (1966).

The deformation predictors are given by:

$$DSH = \partial v/\partial x + \partial u/\partial y$$

$$DST = \partial u/\partial x - \partial v/\partial y$$

$$DEF = (DSH^2 + DST^2)^{1/2}$$

where DSH is the shearing deformation, DST is the stretching deformation, DEF is the total deformation, and u and v are the horizontal wind components in the x and y directions, respectively. Deformation is a quantifiable kinematic predictor that, in effect, acts to strengthen upper-level frontal zones by increasing the horizontal temperature gradients, thereby increasing the likelihood of the generation of SLW by frontal lifting. TI1 and TI2 are computed over specified layers and are given by:

$$TI1 = VWS \times DEF$$

$$TI2 = VWS \times (DEF + CVG)$$

where VWS is the vertical wind (speed) shear and CVG is the horizontal mass convergence computed for the specified layer as given by:

$$CVG = -(\partial u/\partial x + \partial v/\partial y)$$

The TI1 values are in units of 10^{-7} sec^{-2} and range in value from 0 to 15 units. When vertical wind shear is combined with deformation and horizontal convergence in the TI1 and TI2 indices, important predictors are created that simulate the nonlinear interactions among the three predictors and their relationship to aircraft icing. These predictors were selected in the final probability equations.

Many of the predictors offered to the regression procedure were interactive, or combined, predictors including the original formulations of TI1 and TI2 developed by Mancuso and Endlich (1966). Other interactive predictors include the vertical velocity, deformation, and vertical wind shear combined with various synoptic fields, i.e., relative humidity, temperature lapse rate, wind speed, and horizontal convergence. The function of the interactive predictors is partially to account for the particular, diverse, and probably nonlinear combinations of conditions that can lead to the occurrence of the predictand event. The selected variables are expected to interact with or complement one another in predicting the event. Previous studies have shown no clear consensus on the relative order of importance of many of the predictors as related to the occurrence of aircraft icing. In the present work, we are dealing with a very large developmental data sample; therefore, the MOS screening regression procedure should generate stable and reliable statistical relationships between the predictors and the occurrence of icing.

2.4 Unconditional Icing Probability Equations

Linear screening regression and the MOS approach were used to develop forecast equations that give the unconditional probability of aircraft icing for both the warm (March 16 - September 30) and cool seasons (October 1 - March 15). The analysis of icing reports and forecast model fields was limited to the grid blocks within the contiguous U.S. landmass; no over-water grid blocks were used in the regression procedure. The forecasts produced from the resulting equations represent the unconditional probability of aircraft icing intensities of category 4 or greater in 48-km grid blocks during the 2-8, 8-14, 14-20, and 20-26 h periods following 0000 and 1200 UTC. Separate forecast equations were developed for the eastern and western U.S. The two regions are separated by the meridian running along 104 deg west longitude. Each equation was developed from a generalized dataset created by combining data from all grid blocks in each region. Total sample size for the East was about 1.2 million cases (2949 overland grid blocks times 409 sample days) for the 1988-90 cool seasons. For the West, the cool-season sample size was about 0.7 million cases (1728 blocks times 409 days). For the warm season, the sample size was 1.7 million cases for the East and 1.1 million cases for the West. Icing frequency, or the fraction of 48-km grid blocks with icing intensities of category 4 or greater, was generally between 0.1% and 0.7% for the individual 6-h forecast projections during the warm and cool season developmental samples.

Initially, regional 12-term forecast equations were developed for each of the four valid periods following 0000 and 1200 UTC. To enhance forecast consistency, a representative list of 12 predictors was assembled based on individual predictor lists obtained from the separate runs for the eastern and western U.S. The screening regression procedure was then repeated to develop the operational equations by forcing selection of these 12 predictors, thereby, helping to enhance forecast consistency from one valid period to the next. Table 1 shows the 12 predictors in the cool-season icing forecast equations for the eastern and western United States for the low-band region (at or below 15,000 ft) for the four 6-h projections. The predictors in Table 1 are listed in the order of importance in terms of their contribution to the cumulative reduction of variance. The leading predictor for both East and West is relative humidity. In the East, the vertical stratification of temperature and moisture is of prime importance to the occurrence of SLW, followed by contributions from predictors that reflect atmospheric dynamics, i.e., 700-mb relative vorticity, 950-mb height, 500-mb equivalent potential vorticity, and the 300-mb vertical wind shear times wind speed. In the western U.S., contributions from relative humidity and temperature distributions are modified by contributions from terrain-induced vertical motions, moisture convergence, wind shear, wind speed, and the TI1 and TI2 indices, reflecting the importance of atmospheric dynamics related to the underlying topography in the West.

3. RELIABILITY OF FORECASTS

As previously noted, icing frequencies were

Table 1. NGM predictors in cool season MOS probability equations for category 4 or greater aircraft icing in the low-band for the 2-8 h, 8-14 h, 14-20 h, and 20-26 h projections following 0000 and 1200 UTC.

Eastern U.S.	Western U.S.
700-mb relative humidity	850-mb relative humidity
700-mb relative vorticity	1000-500 mb mean relative humidity
300-500 mb temperature difference	850-950 mb TI2 index
Height of freezing level	500-mb terrain-induced vertical velocity
950-mb height	300-mb terrain-induced vertical velocity
850-mb relative humidity	850-mb TI1 index
500-mb equivalent potential vorticity	850-1000 mb temperature difference
700-850 mb equivalent potential temperature difference	950-mb moisture convergence
700-mb temperature minus dew point	850-mb moisture convergence
700-1000 mb temperature difference	850-mb temperature minus dew point
500-700 mb equivalent potential temperature difference	950-500 mb wind (speed) shear
300-mb vertical wind shear times wind speed	850-mb wind speed

less than 1% for the individual 6-h forecast projections resulting in a probability range of about 0 to 4% and 0 to 1.4% for the low-band and high-band MOS forecasts, respectively. Therefore, for ease of use, probabilities for category 4 or greater icing were scaled by multiplicative factors of 20 and 60 for the low band and high band, respectively. As a result, the scaled probabilities for both bands roughly correspond to a range of 0 to 100%. Hereafter, use of the term "probability" refers to the scaled probability values. The reliability or bias of the operational icing equations was evaluated by producing forecasts on the dependent data and then computing frequencies for several icing probability categories, where the scaled values range from 0-10%, 10-20%,...etc. To compute the frequency for each of the scaled forecast categories, the total number of observed grid blocks with icing intensities of 4 or greater in each forecast category was divided by the total number of daily forecasts or grid blocks in that category. For example, the reliability of the cool season probability forecasts for category 4 or greater icing for the 20-26 h projection for the low-band region is shown in Fig. 1. The data points are located at the average scaled forecast probability for each of the categories. The number of forecasts (plotted in thousands) is also shown next to each data point. The unlabeled diagonal line represents perfect forecast reliability or zero bias. Figure 1 indicates that the icing probability forecasts were reasonably reliable for the 1988-90 dependent data sample with a slight tendency to underforecast in the highest probability categories. Similar verification statistics were obtained for the remaining forecast projections in the dependent data sample. Based on our experience in testing other MOS

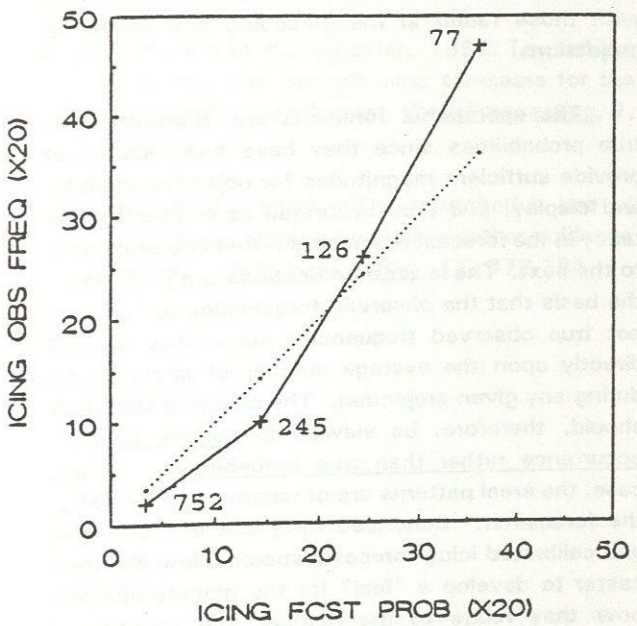

Figure 1. Reliability diagram for cool-season MOS icing forecasts for 20-26 h interval after 0000 UTC. The scaled forecasts are valid for the low-band region. Number of cases (thousands) is plotted next to data points for each category.

forecast equations on dependent data, we anticipate no significant degradation in the verification statistics for independent data samples.

4. FORECAST CONSIDERATIONS

Significant diurnal variations in the magnitude of the probabilities from one 6-h interval to the next were found in the initial test forecasts due to the temporal variability in the reported icing events. Relatively low frequencies are reported at night, for example, during the 2-8 h interval after 0000 UTC and the 14-20 h interval after 1200 UTC (9 p.m. to 3 a.m. EST) when relatively few aircraft are aloft. In contrast, the highest icing frequencies are reported during daylight hours for the 14-20 h interval following 0000 UTC and the 2-8 h interval after 1200 UTC (9 a.m. to 3 p.m. EST) when aircraft traffic is at a maximum. In effect, the icing forecasts give the probability of icing being reported during each of the forecast projections. To compensate for the pronounced diurnal variability, the forecasts for the 1400 to 2000 UTC (maximum reported icing frequency) and 0200 to 0800 UTC (minimum reported icing frequency) forecast projections were calibrated to ensure consistency with the magnitudes of the probability forecasts for the remaining forecast projections. The calibration procedure preserves the forecast patterns for the adjusted intervals and simply modifies the magnitudes to be consistent with those found in the preceding and following projections.

The operational forecasts are, therefore, not true probabilities since they have been scaled to provide sufficient magnitudes for objective analysis and display, and then calibrated to ensure consistency in the forecast magnitudes from one projection to the next. The latter modifications are justified on the basis that the observed frequencies of icing are not true observed frequencies since they depend directly upon the average number of aircraft aloft during any given projection. The modified forecasts should, therefore, be viewed as indices of icing occurrence rather than true probabilities. In any case, the areal patterns are of paramount interest to the forecaster. Continued daily use of the scaled and calibrated icing forecasts should allow the forecaster to develop a "feel" for the magnitudes and how they relate to the number and severity of observed aircraft icing. In effect, the magnitude of the scaled icing forecasts is not nearly as important as the ability to accurately delineate the potential areal extent of significant icing. In practice, scaled threshold values will be subjectively determined based on the day-to-day experience of operational forecasters at AWC in their preparation of operational AIRMETS and SIGMETS. Selection of appropriate threshold values should result in objectively determined areas of expected icing similar in size to those on manual products issued by operational forecasters.

The NGM-based MOS forecasts of aircraft icing should be operationally useful to the forecaster for several reasons. Use of lightning data, for example, to remove convectively-generated icing results in a predictand sample that adheres more closely to the desired predictand for nonconvective icing, which should result in better statistical relationships with the NGM predictors. Use of relatively small (48 km) grid blocks allows the forecast equations to locate and define icing maxima with fairly good resolution, as shown, for example, by the narrow band of scaled forecast values across northern Illinois, Indiana, and Ohio in Fig. 2. The MOS forecast in Fig. 2 corresponds to contours indicating a scaled (actual) range of 0% to 65% (0% to 3.25%) for the icing forecasts. Finally, the relatively large 3-year sample of predictor and predictand data should result in stable and accurate forecast equations. As is the case with all MOS forecasts, however, the new

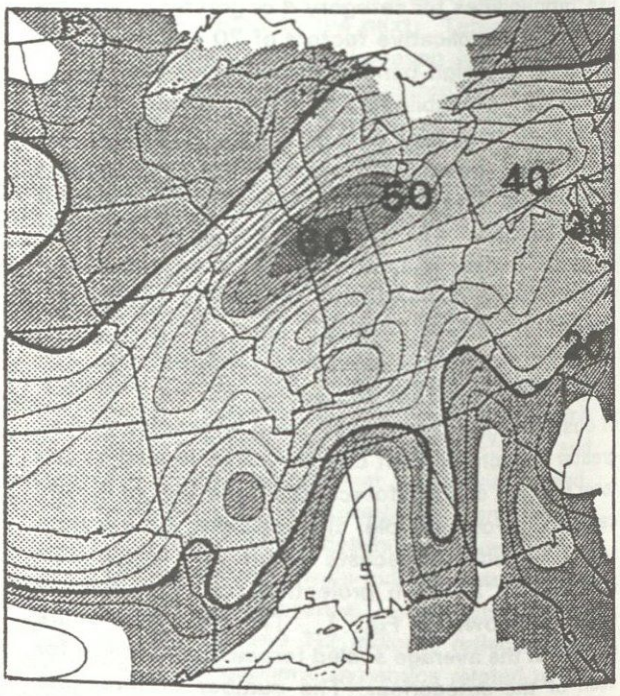

Figure 2. Low-band scaled (x 20) probability contours for category 4 or greater icing in 48-km grid blocks during the 8-14 h projection following 0000 UTC on December 19, 1995.

NGM-based icing forecasts are highly dependent upon the accuracy of the NGM forecasts used as input. Therefore, the guidance may have to be used with caution if the forecaster detects possible errors in the model predictions.

5. GRAPHICS PRODUCTS

The MOS scaled forecasts of aircraft icing will be generated twice daily at NCEP starting with the 1996-97 cool season. The output files are transmitted as graphical files to AWC in Kansas City, Missouri. The files are subsequently unpacked and processed for display on AWC's N-AWIPS communications system by using the NTRANS graphical user interface. Within the context of the N-AWIPS system, the graphical icing products can be animated or looped as desired. Combined displays can also be generated with the icing forecasts and selected meteorological fields, such as the 850-mb relative humidity forecasts, etc., appearing on the same display. These options can be controlled by the forecaster to achieve maximum utility of the graphical icing displays.

6. REFERENCES

George, J. J., 1960: Weather Forecasting for Aeronautics. Academic Press, 673 pp.

Glahn, H. R., and D. A. Lowry, 1972: The use of Model Output Statistics (MOS) in objective weather forecasting. J. Appl. Meteor., 11, 1203-1211.

Hoke, J. E., N. A. Phillips, G. J. Dimego, J. J. Tuccillo, and J. G. Sela, 1989: The regional analysis and forecast system of the National Meteorological Center. Wea. Forecasting, 4, 323-334.

Krider, E. P., R. C. Noggle, and M. A. Uman, 1976: A gated wideband magnetic direction finder for lightning return strokes. J. Appl. Meteor., 15, 301-306.

Mancuso, R. L., and R. M. Endlich, 1966: Clear air turbulence frequency as a function of wind shear and deformation. Mon. Wea. Rev., 94, 581-585.

Miller, R. C., 1972: Notes on analysis and severe storm forecasting procedures of the Air Force Global Weather Central. Air Weather Service Tech. Rep. 200 (Rev.), U.S. Air Force, 102 pp.

Modica, G. D., S. T. Heckman, and R. M. Rasmussen, 1994: An application of an explicit microphysics mesoscale model to a regional icing event. J. Appl. Meteor., 33, 53-64.

Reap, R. M., 1996: Probability forecasts of clear-air turbulence for the contiguous U.S. Preprints Thirteenth Conference on Probability and Statistics in the Atmospheric Sciences, San Francisco, Amer. Meteor. Soc., 66-71.

Rotunno, R., and J. Klemp, 1985: On the rotation and propagation of simulated supercell thunderstorms. J. Atmos. Sci., 42, 271-292.

Schultz, P., and M. K. Politovich, 1992: Toward the improvement of aircraft-icing forecasts for the continental United States. Wea. Forecasting, 7, 491-500.

Schwartz, B. E., 1996: The quantitative use of PIREPS in developing aviation weather guidance products. Wea. Forecasting, 11, 372-384.